Supporting information

Electrochemo-mechanical Failure in Cobalt-Free High-Nickel Cathodes: Common Degradation of Polycrystalline and Single-Crystal Morphologies in Halide-Based All-Solid-State Batteries

Chenxi Song, Mingqian Yu, Yaoyu Ren*, Yang Lu, Qingyun Zhang, Yang Shen*

C. Song, M. Yu, Prof. Y. Ren, Prof. Y. Shen

State Key Laboratory of New Ceramics and Fine Processing

School of Materials Science and Engineering

Tsinghua University, Beijing 100084, China

E-mail: renyaoyu@mail.tsinghua.edu.cn; shyang_mse@mail.tsinghua.edu.cn

Y. Lu, Q. Zhang

China North Vehicle Research Institute, Beijing 100072, China

Materials Synthesis

The PC-NM91 and SC-NM91 cathodes were prepared through a solid-state calcination process. For PC-NM91 preparation, the $Ni_{0.9}Mn_{0.1}(OH)_2$ precursor (YouyanTech Co., Ltd.) was ground with $LiOH·H_2O$ at the molar ratio of 1:1.03. The mixture was then calcined at 770 ℃ for 12 h under an oxygen atmosphere to gain an optimal ordered crystalline structure. The SC-NM91 sample was synthesized by the same precursor mixed with $LiOH·H_2O$ at a molar ratio of 1:1.05, followed by calcination at 920 ℃ for 2 h, firstly, and 700 ℃ for 12 h under an oxygen atmosphere. The solid-electrolyte Li_3InCl_6 and LiPSCl were purchased from Canrd.

Materials Characterization

The cathode crystal structure was analyzed by X-ray diffraction (Rigaku, D/max-2550) using Cu Kα radiation in the 2θ range of 5-130° with a 0.02° step size. The lattice parameters and the Li/Ni mixing degree were obtained from XRD data by Rietveld refinement using Fullprof software. Scanning electron microscopy (SEM, Zeiss Merlin Compact) was used for morphological characterization. The samples for cross-sectional SEM analysis were prepared by ion beam slope cutter (Leica EM TIC 3X). The cycled cathode and pristine Li_3InCl_6 was investigated by X-ray photoelectron spectroscopy (XPS, Thermofisher Escalab 250XI), and the standard C 1s peak (284.8 eV) was used to calibrate the whole spectrum of the sample. The particle size distribution of the as-prepared samples was analyzed using a laser diffraction particle size analyzer (Malvern, MS2000). The specific surface area was determined by nitrogen adsorption-desorption tests using a physical adsorption instrument (Quantachrome, SI-MP).

Electrochemical Measurements

The Fabrication of Liquid-Electrolyte Batteries: The cathode was prepared by mixing the NM91 powder, polyvinylidene fluoride (PVDF) binder, and carbon black additive with a mass ratio of 8:1:1 in N-methyl-2-pyrrolidone (NMP) solvent and drying at 80 °C under vacuum for 12 h. The full cells were assembled with a lithium disk as anode and a Celgard 2325 separator into CR-2025 coin cell cases in a glovebox under an inert atmosphere. The loading of the cathode is approximately 4 mg/cm^2. The electrolyte was 1 mol L^{-1} $LiPF_6$ dissolved in ethylene carbonate (EC) and dimethyl carbonate (DMC) (EC: DMC = 3:7 by volume) with 2% vinylene carbonate (VC).

The Fabrication of All-Solid-State Batteries: The NM91 powder was mixed with VGCF, and Li_3InCl_6 solid electrolyte with a weight ratio of 63:1:36 or 53:1:46 by using a pestle and mortar for 30 min to obtain the cathode composites. 50 mg Li_3InCl_6 powder was pressed into a pellet with a pressure of 125 MPa, and then 30 mg of LiPSCl powder was spread and pressed at 125 MPa. The cathode composite was pressed on the side of the Li_3InCl_6 pellet with a mass loading of 5 mg/cm^2 at 500 MPa. Afterward, $Li_{0.5}In$ metal foil was attached to the LiPSCl side and pressed at 125 MPa. The ASSBs were evaluated at the voltage window of 3.0-4.3 V (vs. Li^+/Li), and a stack pressure of 125 MPa was applied.

Electrochemical impedance spectroscopy was conducted from 1 MHz to 10 mHz with an applied AC

potential amplitude of 10 mV. For the re-pressurization test, the cycling was paused, and the pressure was reset to 125 MPa to compensate for any potential pressure relaxation in the fixture before the subsequent EIS measurement. The galvanostatic intermittent titration technique (GITT) was used to test the Li+ diffusion coefficient, and all samples were measured with a galvanostatic current set to 0.1 C, the charge or discharge process for 20 min, and a time interval of 90 min close to steady state. In-situ XRD patterns were collected on high-resolution X-ray diffractometer (Empyrean, PANalytical).

Note S1. Calculation of Electronic Percolation Threshold based on Effective Medium Theory (EMT)

To verify the robustness of the electronic network, the percolation threshold(Φ_c) for the high-aspect-ratio vapor-grown carbon fibers (VGCF) in the cathode composites was calculated using Effective Medium Theory (EMT) with a 1D-shape correction[1]. According to the classical model for randomly oriented fiber-like fillers, Φ_c is primarily determined by the aspect ratio (a = length/diameter):

$$\Phi_c \approx L_z \approx \frac{1}{a^2}(\ln 2a - 1)$$

For VGCF with a typical aspect ratio of $a \approx 50 - 100$, the theoretical Φ_c is estimated to be 0.04-0.14 vol%. This is significantly lower than the actual VGCF loading in NM91 cathode (approximately 1.6-1.7 vol%), ensuring a highly redundant electronic conduction framework.

Ref [1]: C.-W. Nan, *Progress in Materials Science*, 1993, **37**, 1-116.

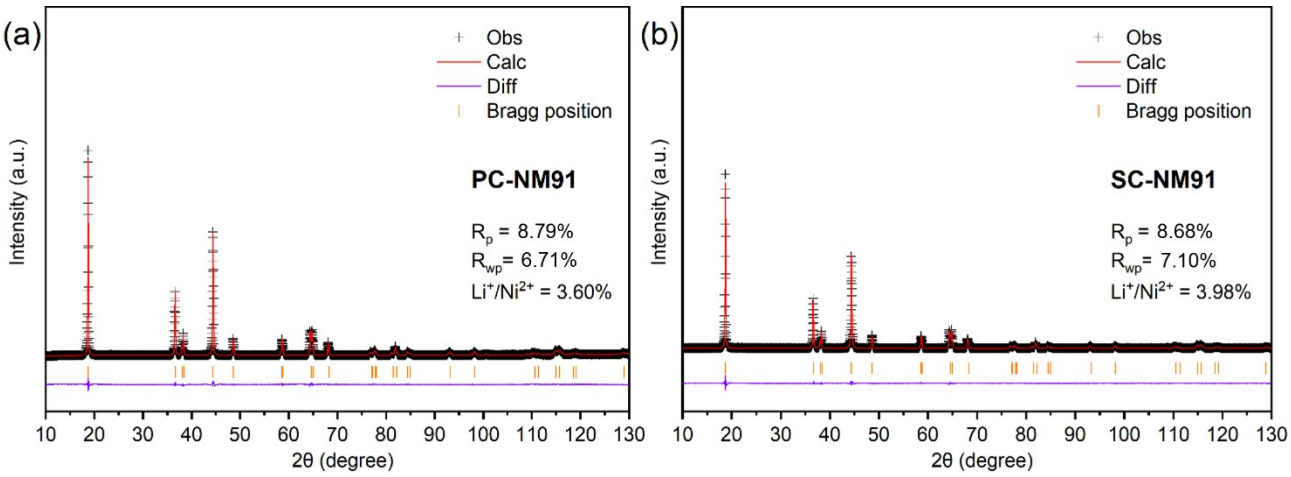

Figure S1. The XRD pattern and Rietveld refinement results of (a) PC-NM91 and (b) SC-NM91.

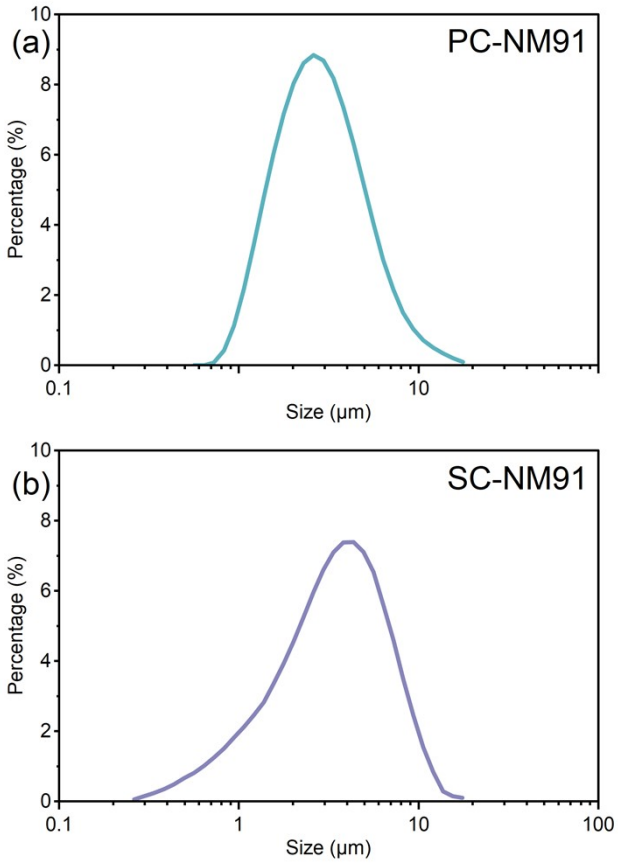

Figure S2. The particle size distribution of (a) PC-NM91 and (b) SC-NM91.

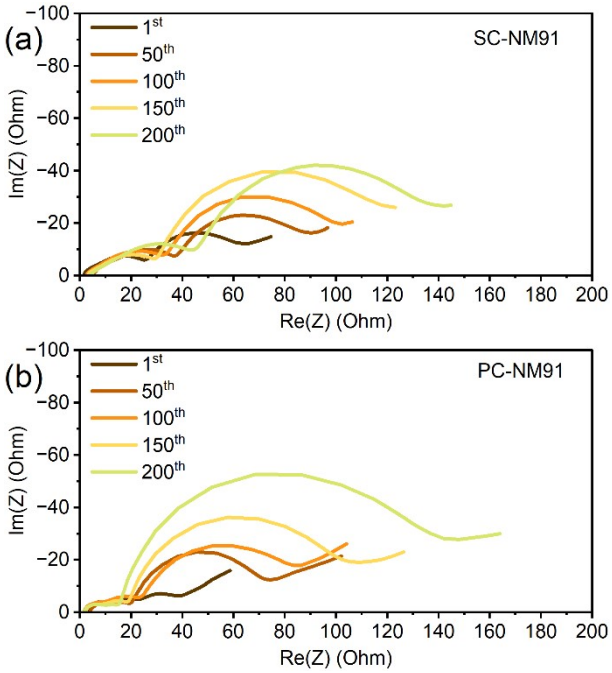

Figure S3. Nyquist plots of the electrochemical impedances measured at 4.3 V at every 50th cycle for (a) SC-NM91, (b) PC-NM91.

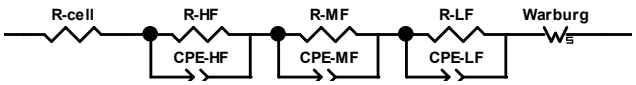

Figure S4. Corresponding equivalent circuit model for Nyquist plots analysis in Figure S3.

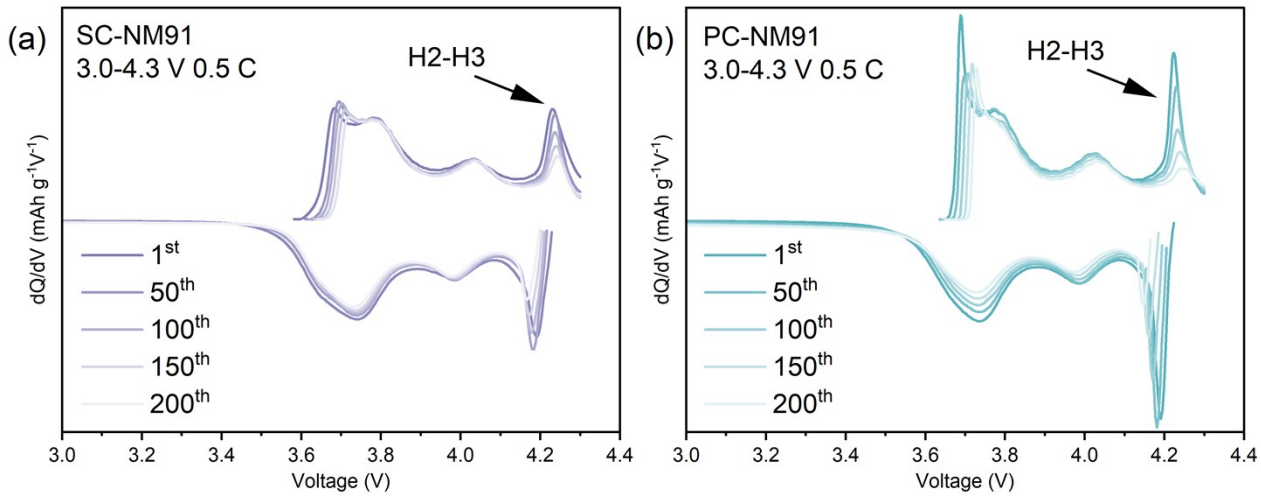

Figure S5. (a) SC-NM91 and (b) PC-NM91 cathodes derived by differentiating the charge-discharge curves during cycling.

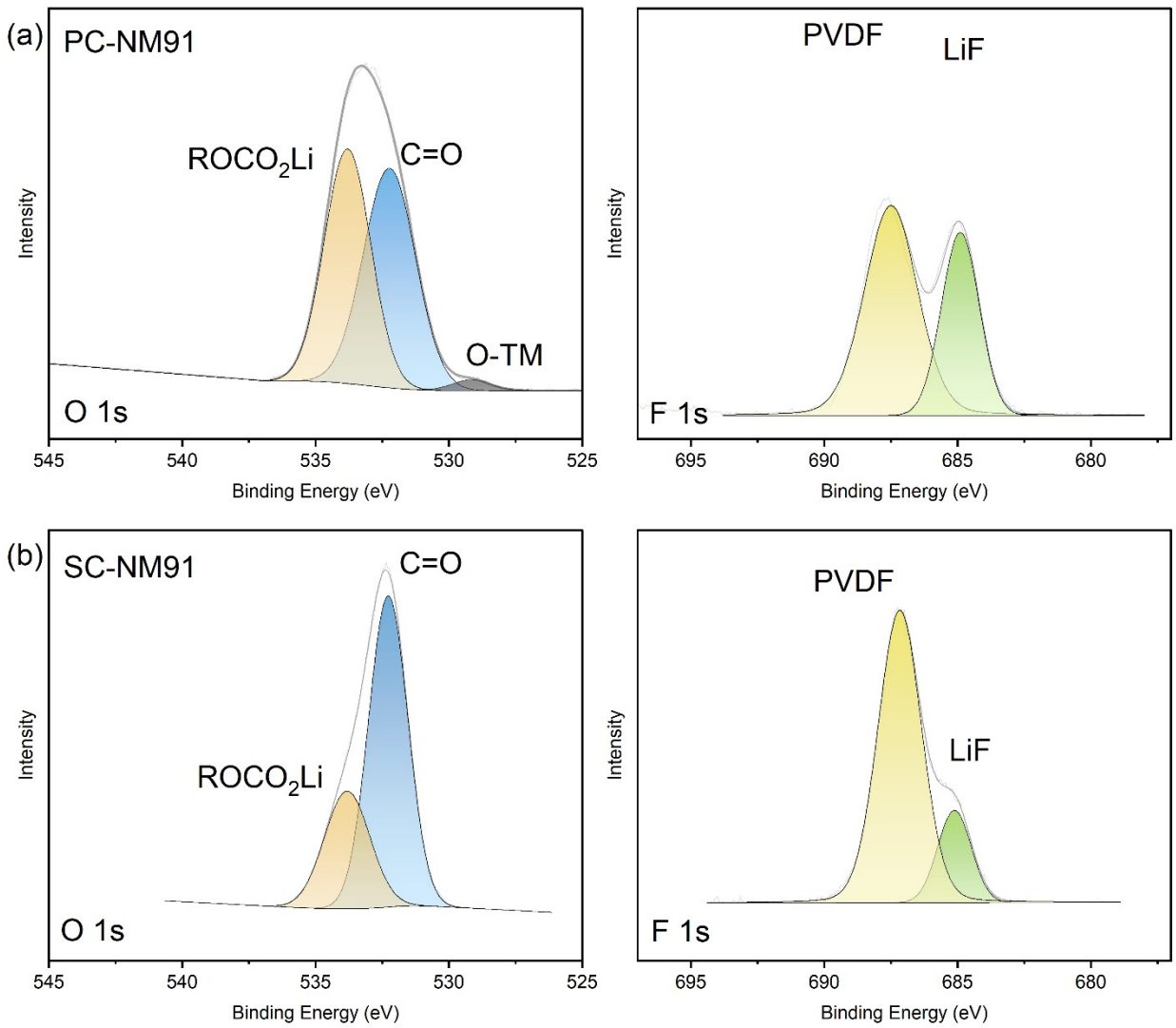

Figure S6. The XPS results of O 1s and F 1s for cycled (a) PC-NM91 and (b) SC-NM91. Plot of PC-NM91 is generated based on data reported in our previous work.[2]

Ref [2] C. Song, Y. Ren, L. Gu, Q. Zhang, Y. Lu and Y. Shen, J. Mater. Chem. A, 2025, 13, 26627-26636.

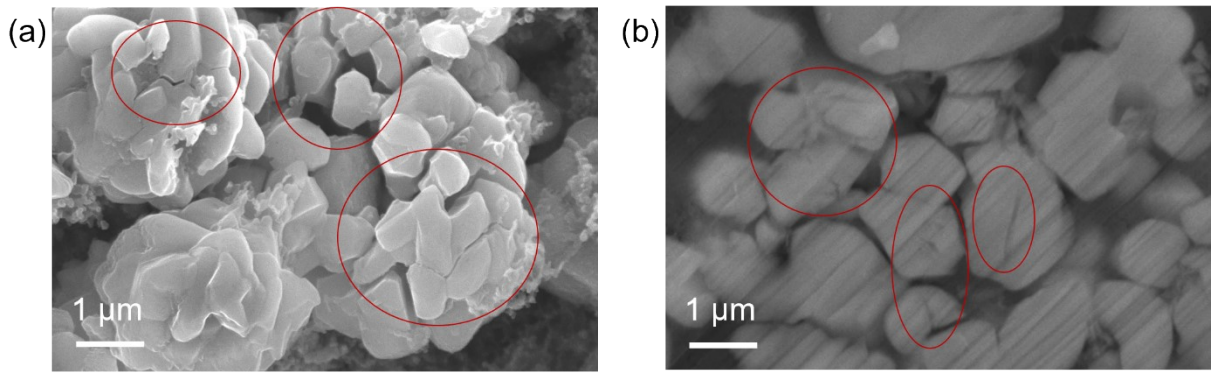

Figure S7. The SEM images of cycled (a) PC-NM91 and (b) SC-NM91, the intergranular and intragranular cracks are circled in red.

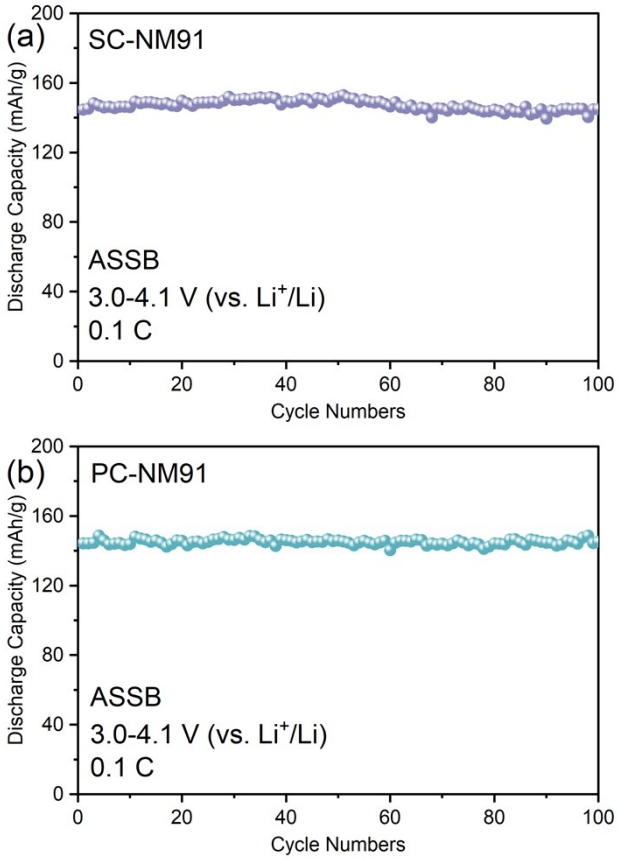

Figure S8. The cycling performance of (a) SC-NM91 and (b) PC-NM91 with an upper voltage of 4.1 V.

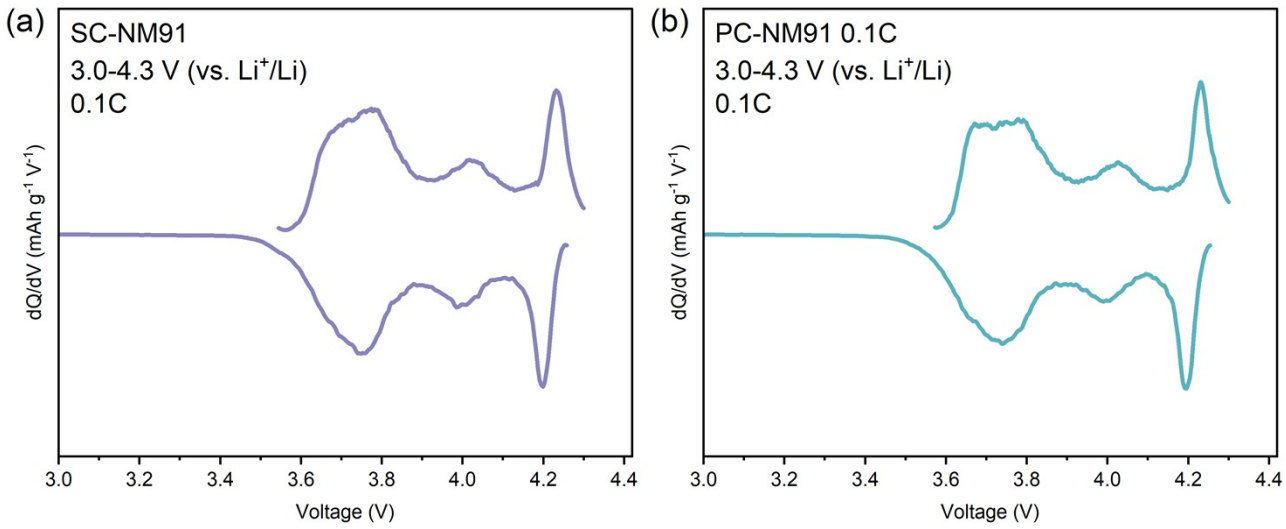

Figure S9. The dQ/dV curves for (a) SC-NM91 and (b) PC-NM91 at 0.1 C rate.

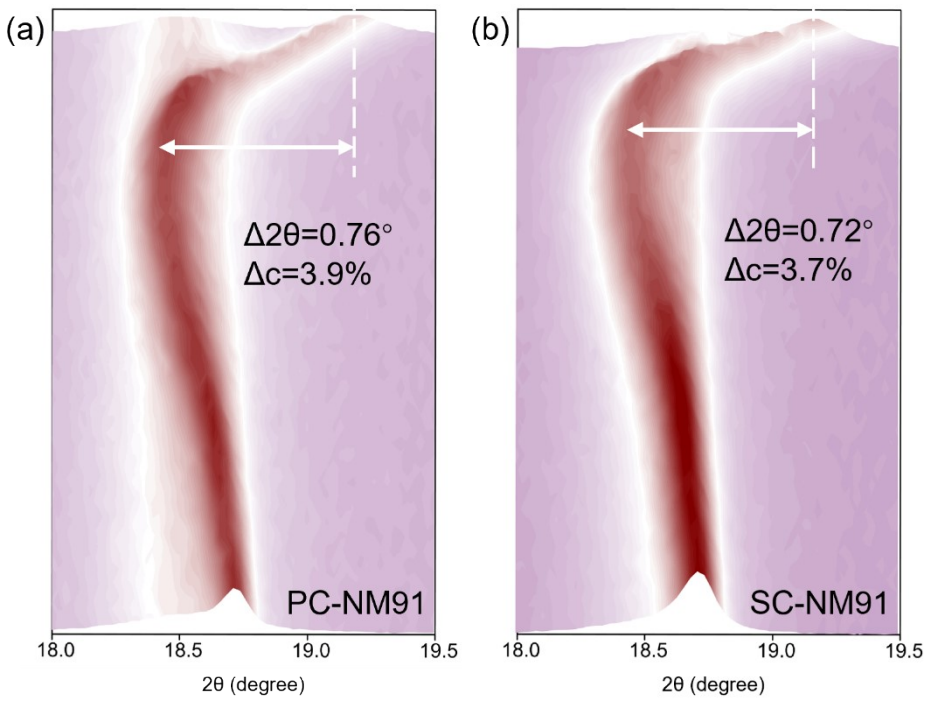

Figure S10. In-situ XRD contour plots of the (003) reflection for (a) PC-NM91 and (b) SC-NM91 cathodes during the first charge process to 4.3 V at 0.1 C rate.

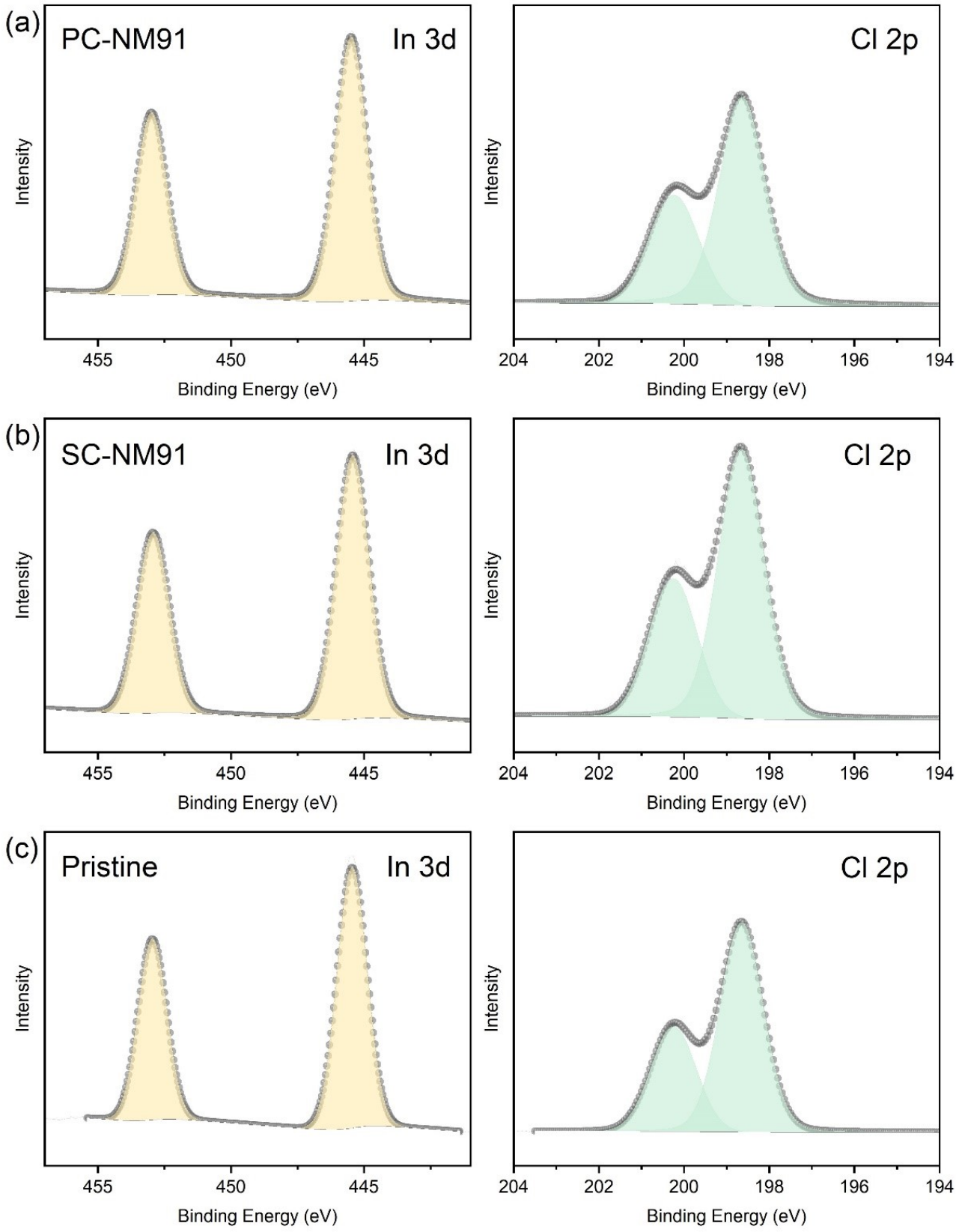

Figure S11. XPS spectra of In 3d and Cl 2p peaks of (a) PC-NM91 and (b) SC-NM91 composite cathodes after 100 cycles at 0.1 C, and (c) pristine Li_3InCl_6.

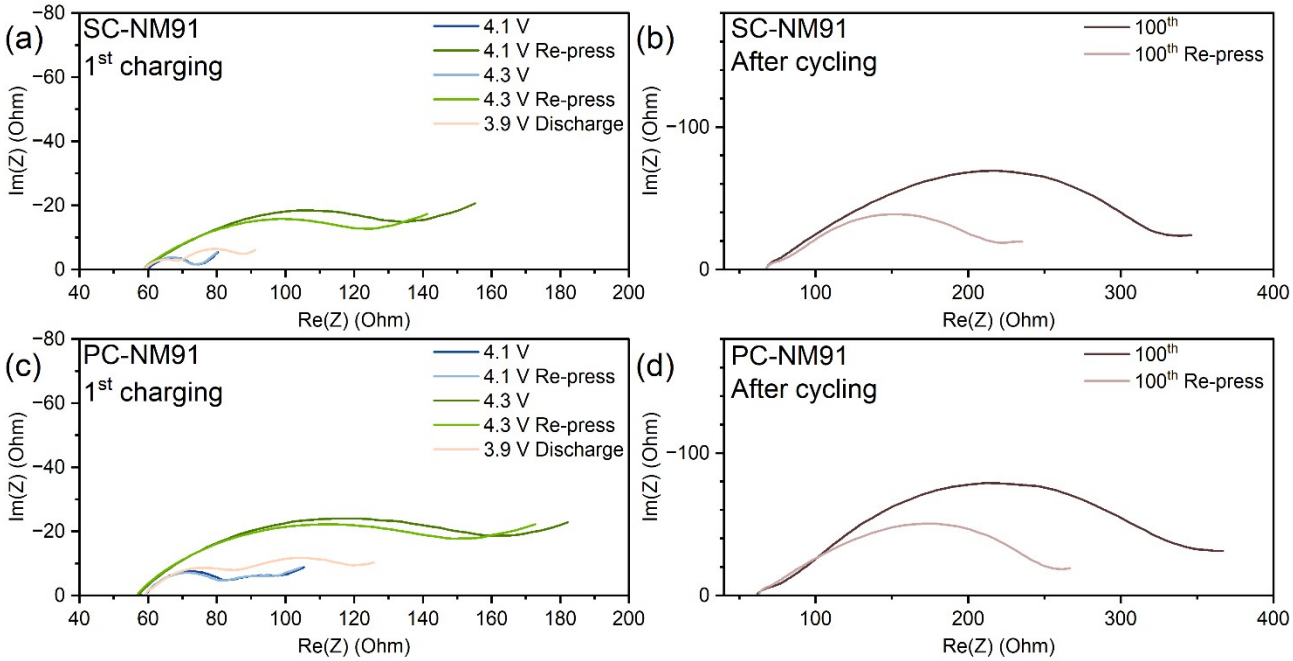

Figure S12. Nyquist plots of the electrochemical impedances measured at the first charging process for (a) SC-NM91, (c) PC-NM91 at different SOC, with re-pressurization experiments. Nyquist plots of the electrochemical impedances measured at 4.3 V after 100 cycles at 0.1 C for (b) SC-NM91, (d) PC-NM91 with re-pressurization experiments.

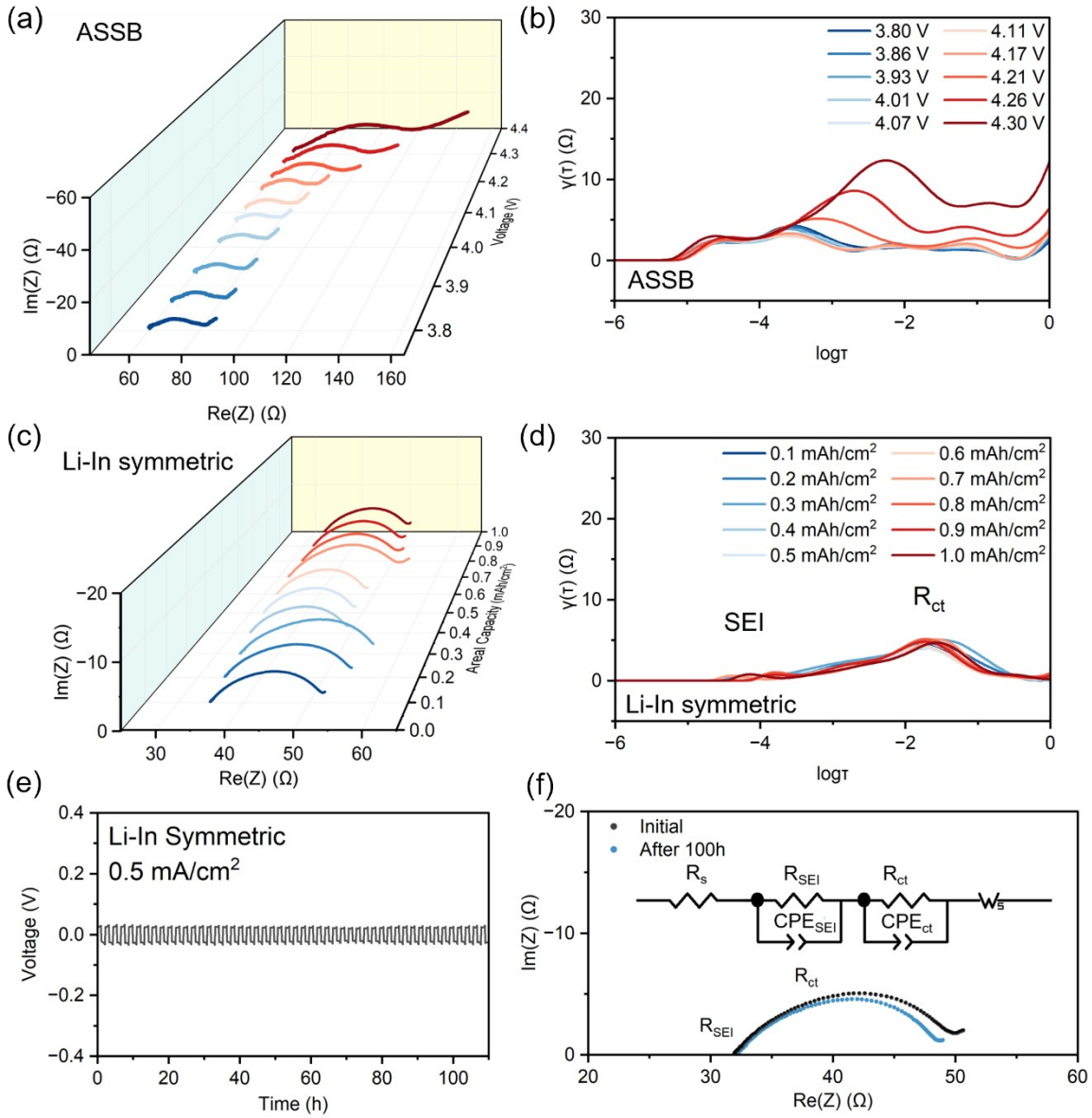

Figure S13. (a) Nyquist plots and (b) DRT curves of the ASSB at different charge voltages ranging from 3.8 V to 4.3 V. (c) Nyquist plots and (d) DRT analysis of the Li-In symmetric cell towards 1 mAh/cm^2 areal capacity. (e) Galvanostatic cycling performance of the Li-In symmetric cell at a current density of 0.5 mA/cm^2. (f) Nyquist plots of the Li-In symmetric cell before and after 100 h of cycling, with the inset showing the equivalent circuit model used for impedance fitting.

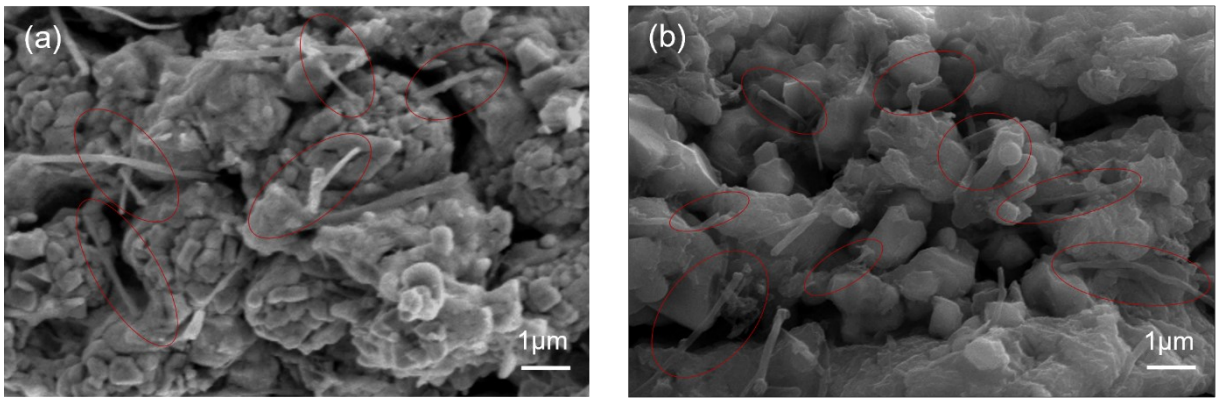

Figure S14. Representative SEM images of the cycled cathode. Red circles indicate the carbon network bridging the gaps formed induced by stress relaxation.

Table S1. Rietveld refinements of the XRD patterns for SC-NM91 and PC-NM91 cathodes

SC-NM91	**atom**	**site**	**X**	**Y**	**Z**	**Occ**
a = 2.8760 Å	Li	3a	0	0	0	0.0801
c = 14.2102 Å	Ni	3a	0	0	0	0.0033
Volume: 101.8 $Å^3$	Ni	3b	0	0	0.5	0.0717
Rp = 8.68%	Mn	3b	0	0	0.5	0.0083
Rwp = 7.10%	Li	3b	0	0	0.5	0.0032
Li/Ni: 3.98%	O	6c	0	0	0.2418	0.1667
PC-NM91	**atom**	**site**	**X**	**Y**	**Z**	**Occ**
a = 2.8760 Å	Li	3a	0	0	0	0.0804
c = 14.2082 Å	Ni	3a	0	0	0	0.0030
Volume: 101.8 $Å^3$	Ni	3b	0	0	0.5	0.0720
Rp = 8.79%	Mn	3b	0	0	0.5	0.0083
Rwp = 6.71%	Li	3b	0	0	0.5	0.0030
Li/Ni: 3.60%	O	6c	0	0	0.2418	0.1667

Table S2 The particle size distribution results from the laser particle sizer measurements.

	D10 (μm)	D50 (μm)	D90 (μm)
PC-NM91	1.35	2.60	5.55
SC-NM91	1.07	3.16	6.80

Table S3 Nitrogen adsorption and desorption test results for NM91 materials.

	Surface area (m^2/g)
PC-NM91	1.218
SC-NM91	0.625